

Characterization of glass beads by image methods for pavement marking retroreflectivity

Caracterização de microesferas de vidro para retrorrefletividade de sinalização horizontal por técnicas de imagens

Laura Nascimento Mazzoni¹, Deise D. N. Machado², Kamilla L. Vasconcelos³,
Liedi L. B. Bernucci⁴, Guilherme R. Linhares⁵, Verônica T. F. Castelo Branco⁶

¹University of São Paulo, São Paulo – Brazil, laura.mazzoni@usp.br

²Technology Faculty of São Paulo – Brazil, deisedias.projetos@gmail.com

³University of São Paulo, São Paulo – Brazil, kamilla.vasconcelos@gmail.com

⁴University of São Paulo, São Paulo – Brazil, liedti@usp.br

⁵University of São Paulo, São Paulo – Brazil, guilherme.linhares@arteris.com.br

⁶Federal University of Ceará, Ceará – Brazil, veronica@det.ufc.br

Recebido:

16 de março de 2021

Aceito para publicação:

17 de janeiro de 2022

Publicado:

6 de agosto de 2022

Editor de área:

Jorge Barbosa Soares

Keywords:

Shape characterization.

CamSizer.

AIMS.

Test site.

Palavras-chave:

Caracterização de forma.

CamSizer.

AIMS.

Trecho experimental.

DOI:10.14295/transportes.v30i1.2584

ABSTRACT

Road safety is a worldwide concern. Traffic injuries are the main cause of death for children and young people. One alternative to improve traffic safety is the enhancement of pavement markings visibility. Pavement marking efficiency depends on day and night visibility. Nighttime visibility (retroreflectivity) occurs due to the presence of glass beads. This paper compares the performance of two glass beads: G1 – Brazilian glass bead produced with recycled glass; and G2 – imported glass bead produced with new material. The research evaluated the retroreflectivity decrease of a test deck using two water-based paints from different manufacturers. The glass beads characterization process used the Computerized Optical Equipment (COE), CamSizer, and the Aggregate Image Measurement System (AIMS) to evaluate the shape, size, and gradation. Results indicated different retroreflectivity decrease trends for pavement markings with distinct glass beads, which could be associated with their shape characteristics and grain size distribution. The glass beads G1 presented the worst shape properties which lead to the poorest retroreflectivity at the test site. Thus, image characterization is helpful in estimating markings retroreflectivity prior to its application. Therefore, G1 cannot be used to substitute G2, regarding the retroreflectivity requirements in Brazil.

RESUMO

A retrorrefletividade da sinalização horizontal ocorre devido à presença de microesferas de vidro. Esse trabalho tem como objetivo comparar o desempenho de duas microesferas: G1 – nacional, produzida a partir de vidro reciclado; e G2 – importada, produzida com vidro virgem. O trabalho avaliou a retrorrefletividade de um trecho experimental no qual foram utilizadas duas tintas à base de água de diferentes fabricantes. Os equipamentos utilizados para a caracterização de tamanho e forma das microesferas foram o CamSizer e o *Aggregate Image Measurement System* (AIMS). Os resultados indicaram diferentes tendências para o decaimento da retrorrefletividade, o que foi atribuído às características das microesferas. A microesfera de vidro G1 apresentou propriedades de forma inadequadas, o que resultou na redução da retrorrefletividade. A caracterização por imagem foi útil para estimar a retrorrefletividade antes de sua aplicação em campo. Assim, G1 não pode substituir G2, considerando os requisitos de retrorrefletividade do Brasil.



1. INTRODUCTION AND BACKGROUND

During the last decades, the World Health Organization published several reports presenting the deaths rates and prevention methods for traffic injuries. In 2015, over 1.2 million people died due to road traffic injuries all over the world (WHO, 2015). One of the targets of Sustainable Development Goals of the Organization of United Nations was to halve the number of deaths and injuries by traffic accidents by the year of 2020 (United Nations, 2015). Despite the efforts, deaths by traffic injuries increased to 1.35 million every year and represents the main cause of death among children (age 5 – 14 years) and young people (age 15-29 years) (WHO, 2018).

Traffic safety depends on vehicles characteristics, human behavior, climatic conditions, and the characteristics of the road. Regarding roads characteristics, traffic accidents rates may be reduced by the improvement of pavement markings visibility. Pavement markings are any sign applied to the pavement surface with function to provide guidance and information for road user (FHWA, 2007). Pavement markings must be visible for drivers. During the night, pavement marking's visibility occurs due to the retroreflectivity, an optical phenomenon in which the light is reflected in direction to its source. Researches evaluating the safety effect of pavement markings noticed the decrease in nighttime crash rates with the improvement of the visibility caused by higher values of pavement marking's retroreflectivity (Carlson, Park and Andersen, 2009).

Despite the evidence of traffic accidents reduction, there is no agreement on the minimum retroreflectivity value required but some researchers suggest between 80 to 150 $\text{mcd/m}^2/\text{lx}$ (Carlson, Park and Andersen, 2009). In Brazil, road agencies require that white pavement markings with retroreflectivity value below 120 $\text{mcd/m}^2/\text{lx}$ must be repainted. The retroreflectivity is the main parameter to evaluate pavement marking quality (Mizera, 2008). The retroreflectivity in pavement marking occurs due to an optical phenomenon with the glass beads exposed on the surface as shown by Figure 1.

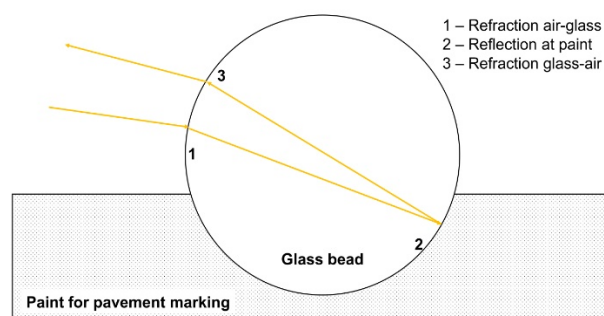


Figure 1. Optics phenomenon occurring during retroreflection

The ability of glass beads to provide the retroreflectivity for pavement markings depends on the raw glass quality and the manufacturing process which affect their properties as gradation, size, coatings, and shape (Migletz, Fish and Graham, 1994). Migletz, Fish and Graham (1994) report that trials of using crushed glass or aluminum and brass spheres for pavement markings were unsuccessful due to their lack of sphericity and transparency, respectively. Based on the findings by Migletz, Fish and Graham (1994) and Figure 1, the ideal glass bead for pavement markings must be a perfect and massive sphere, i.e., the glass bead must present low air inclusion and optimum shape properties. The presence of air bubbles inside the glass beads

would cause additional light refraction and interfere on the light ray's path, causing the reduction of retroreflectivity. Regarding the glass beads shape for both elongation and angularity, the lack of sphericity also causes the retroreflectivity reduction owing to problems on the light reflection angle (Smadi et al, 2013).

During the manufacturing process some glass particles may adhere to each other and form random shapes or even present crushed glass shape causing reduction in pavement markings retroreflectivity values. Standards require minimum percentages of round and spherical particles for pavement markings (AASHTO, 2013a). Fast and accurate methods to characterize glass beads are very important to guarantee quality and durability of pavement markings regarding retroreflectivity. Recently, computerized optical equipment has been used as alternative to traditional methods to evaluate glass bead size and shape (Garboczi and Azari, 2011; Smadi et al, 2014).

Besides glass beads' shape, the beads' density on pavement marking surface has been studied to correlate the percentage of glass bead area covering the pavement marking surface with the retroreflectivity value. This technique was first reported by Rich, Maki and Morena (2002) and they found a strong increasing correlation for the beads content and retroreflectivity value. In addition, the glass beads' embedment depth into the binder film also influences retroreflectivity. The ideal embedment depth ranges from 40% to 60% of particle's diameter. Pavement marking with glass beads embedment depths over 60% present small area exposed to receive the light and the retroreflectivity values tend to reduce. When the glass beads present embedment depths below 40% they tend to present to higher initial retroreflectivity values but they are easily lost due to lack of contact area for the adhesion (Texas DOT, 2004). Therefore, larger glass beads contribute to the improvement of the initial retroreflectivity of pavement markings.

Regarding the embedment depths of glass beads, particles of different diameter can be used for retroreflectivity maintenance. Glass beads' diameters must fit in a range of size distributions specified by standards and must be chosen according to the use (Texas DOT, 2004). The typical diameter of pavement markings' glass beads ranges from 0.180 to 1.700 millimeters. Some glass beads present issue for reaching the proper embedment depth and are easily removed from marking. Therefore, the surface must be treated with an adhesion coating during the manufacture process, covering them with silane which presents chemical affinity with glass from the beads and with the polymeric resin from the binder. Thus, the treatment with silane converts glass bead and binder in a composite material enhancing durability (Texas DOT, 2004).

Besides the adhesion coating, the binder film ageing and wear caused by weather and traffic remove beads from pavement marking, decreasing the retroreflectivity over time (Sathyanarayanan, Shakar and Donnell, 2008; Hummer, Rasdorf and Zhang, 2011). In the U.S.A, the AASHTO evaluates materials quality by monitoring test deck installed transversal to traffic on several regions of the country (NTPEP, 2004). Migletz et al (2001) statistically modeled the durability of marking materials as a function of time and accumulated traffic. They verified that the regression modeling obtained did not fit properly the durability of the same material in distinct test decks. The non-fitness was attributed to the variations on the roadway type, the climatic conditions, the state highway agency specifications, the contractors, and the quality control during the installation.

Pike and Songchitrukka (2015) evaluated the retroreflectivity of transversal and longitudinal test decks. They proposed an exponential statistical model with strong correlation between the

retroreflectivity readings for both test decks and affirmed that the model can be used to predict the retroreflectivity of usual markings by the transversal test deck measures. Test decks are important to evaluate materials' quality and durability. The selection of pavement marking binder must also consider costs and environmental concerns (Babić, Burghardt and Babić, 2015). In this context, water-based paints present satisfactory performance regarding durability, pollutants emissions and costs (Babić, Burghardt and Babić, 2015).

This research has the objective to evaluate the performance of a Brazilian glass bead manufactured with recycled glass and one imported glass bead made of virgin glass. They were compared in laboratory by evaluating shape, size, and gradation properties and in the field by monitoring the retroreflectivity of pavement markings test site highway with very heavy traffic. The test site was constructed using two acrylic water-based paints produced by different manufacturers combined with the two glass beads.

2. MATERIALS CHARACTERIZATION

The pavement markings are complex road elements composed by glass beads and binders. This research assessed the quality of two water-based paints and two glass beads manufacturers.

2.1. Glass beads: adhesion coating

The characterization considering the adhesion coating followed the prescription of the Brazilian standard ABNT NBR 16184 (ABNT, 2013). The method is empirical and qualitative. The test consists in observing the color of a glass bead sample in contact with a solution of 0.01g of potassium permanganate in 100ml of demineralized water. The solution is pink and when it reacts in contact with silane (the adhesion coating) its color changes to brown. The glass bead sample tested must be compared to a reference glass bead known without adhesion coating where the color of the test maintains pink. Figure 2 presents the results for three samples: (a) the reference glass bead, (b) glass bead G1 and, (c) glass bead G2.



Figure 2. Adhesion test for glass beads: (a) Reference glass bead with no adhesion coating treatment, (b) Glass bead G1; (c) Glass bead G2

As presented by Figure 2, the sample with G2 remained pink as well as the reference sample, which indicates the absence of adhesion coating. For sample (b) with G1, the color changed to green-brown, confirming the presence of silane for adhesion coating. The silane is a silicon used for the improvement of adhesion between materials. The presence of silane in G1 indicates that the adhesion of glass beads to the paints film are stronger than other glass beads. Therefore, it is expected that the pavement markings containing glass bead G1 present good retroreflectivity values for a longer period.

2.2. Glass beads: Gradation, size, and shape

The gradations IIA and IIC from Brazilian standard ABNT NBR 16184 (ABNT, 2013) were

selected from each glass bead manufacturer for the performance evaluation. Figure 3 illustrates both gradations range. They were characterized regarding size distribution and shape properties.

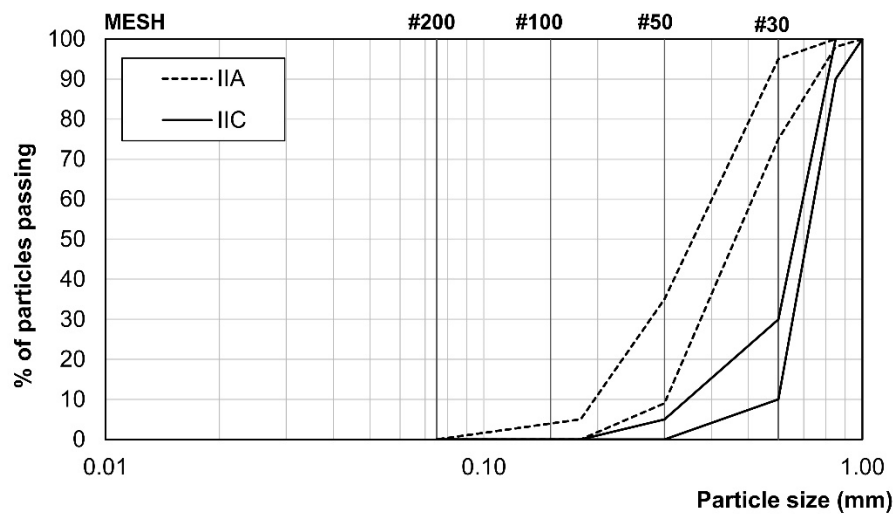


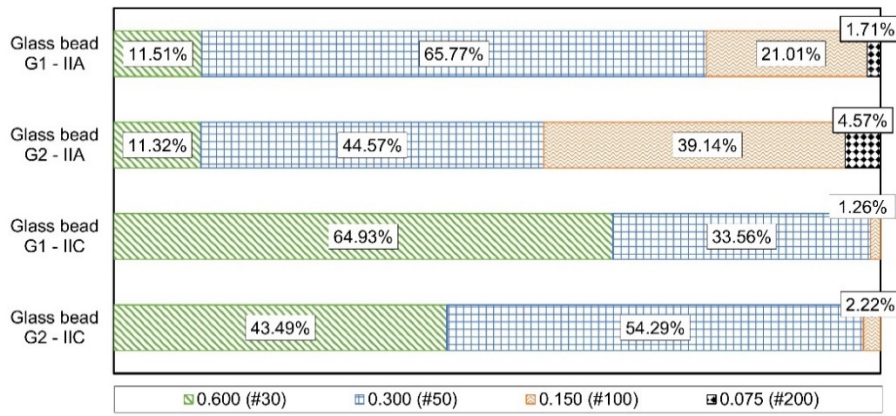
Figure 3. Glass beads' gradation according to the Brazilian specification ABNT NBR 16184 (2013)

The evaluation of shape and size used image techniques that are widely used to analyze particles (Smadi et al, 2014). The present study used two image analysis methods: Computerized Optical Equipment (COE) (AASHTO, 2013b) used to characterize size and shape, and the Aggregate Image Measurement System (AIMS) (AASHTO, 2012) used for aggregates and without previously reported use for glass bead shape characterization.

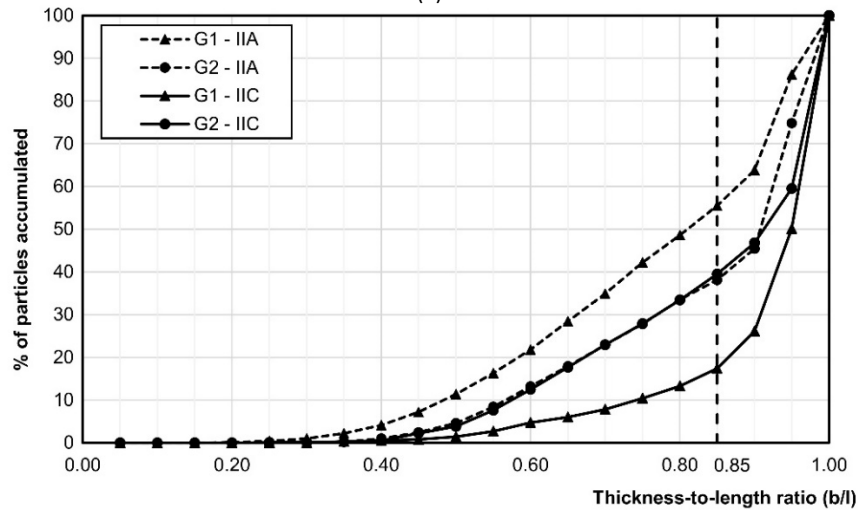
2.2.1. Computerized Optical Equipment (COE)

The computerized optical equipment used was the *CamSizer* by Retsch which analyzes the size distribution and the shape parameters by digital image processing. The particles flow inside the equipment. The experiment is interrupted when parameters' distribution stops changing statistically. There is not a specific or general number of particles evaluated. The two parameters considered to assess glass bead's shape were thickness-to-length ratio (b/l) and sphericity (SPHT). The thickness-to-length ratio (b/l) is the ratio of the major to the minor dimension of the particle. Round particles present b/l around one (1), while elongated particles are around zero (0). The sphericity is calculated as $4\pi A/P^2$, where A is the projected area of the particle and P is the perimeter of each particle. The SPHT quantifies the particle angularity. Angular particles present SPHT around zero (0), and when the particle has smooth surface, SPHT is around one (1). Figure 4 presents the results of size distribution, thickness-to-length ratio, and sphericity for glass beads. According to AASHTO PP74-13, the threshold for round glass beads must be higher than 0.85 for b/l and 0.93 for SPHT.

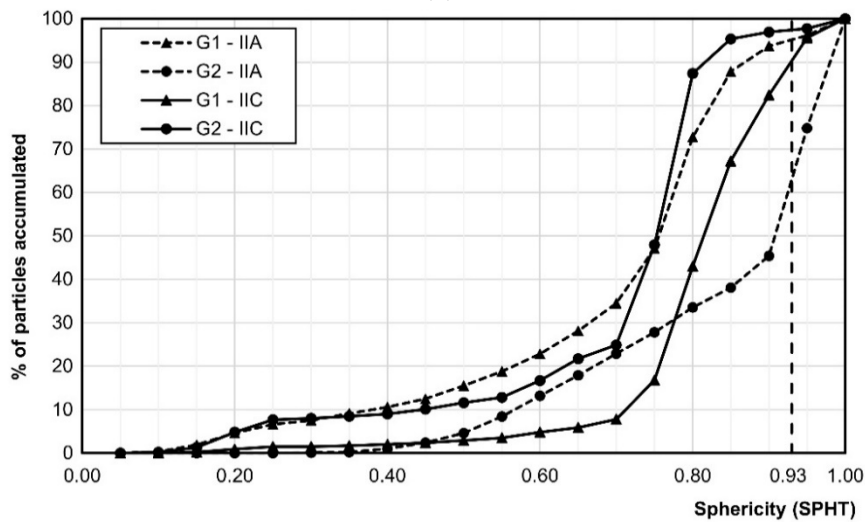
Figure 4(a) illustrates the size distribution considering the retained percentage of particles for each size range. The fractions differ for each manufacturer. The percentage of particles smaller than 0.600 mm for gradation IIA are equal for both manufacturers, but G1 presents 20% more particles between 0.600 mm and 0.300 mm than G2. The same difference occurs for particles bigger than 0.600 mm for gradation IIC. In general, G2 has smaller particles than G1, which can explain why the manufacturer did not used adhesion coating once smaller particles tend to present better embedment depth.



(a)



(b)



(c)

Figure 4. CamSizer results: (a) Size distribution, (b) Thickness-to-length ratio distribution for glass beads with threshold of 0.85; (c) Sphericity distributions for glass beads with threshold of 0.93

Figure 4(b) shows the distribution of thickness-to-length ratio for all glass beads. Regarding the threshold of 0.85, the percentage of round particles are very distinct for G1 gradations. Only 44.5% of particles present b/l over 0.85 for G1-IIA, whereas 82.6% of G1-IIC particles present b/l over 0.85. However, both G2 gradations are very similar with around 60% of particles acceptable. The similarity for G2 can be attributed to the size distribution, since both

gradations present most particles retained at sieve #50, while for G1, each gradation presents a different sieve retaining most particles. Therefore, the difference of acceptable particles can be attributed to their size, which can affect the shape properties regarding elongation, since smaller particles tend to be more elongated than bigger beads.

Figure 4(c) displays the sphericity results for all glass beads. Regarding the threshold of 0.93, all beads present poor shape properties. G2-IIA present the best sphericity of all materials, with around 45% of particles considered as round. Even though, this percentage is very low since most beads are non-spherical. All the other beads sample have less than 15% of round particles.

Both parameters indicate shape properties (elongation and angularity), but their results were very distinct. For SPHT, less than half of particles could be considered as spheres, while for b/l most of them were above the threshold, which may indicate that particles are round but their surface are not very smooth. The divergent and complex results lead to investigate particles' shape with another image tool that was not previously used for glass beads' shape analysis. The method chosen was the Aggregate Image Measurement System (AIMS) since the equipment is used to characterize aggregates for asphalt mixtures.

2.2.2. Aggregate Image Measurement System (AIMS)

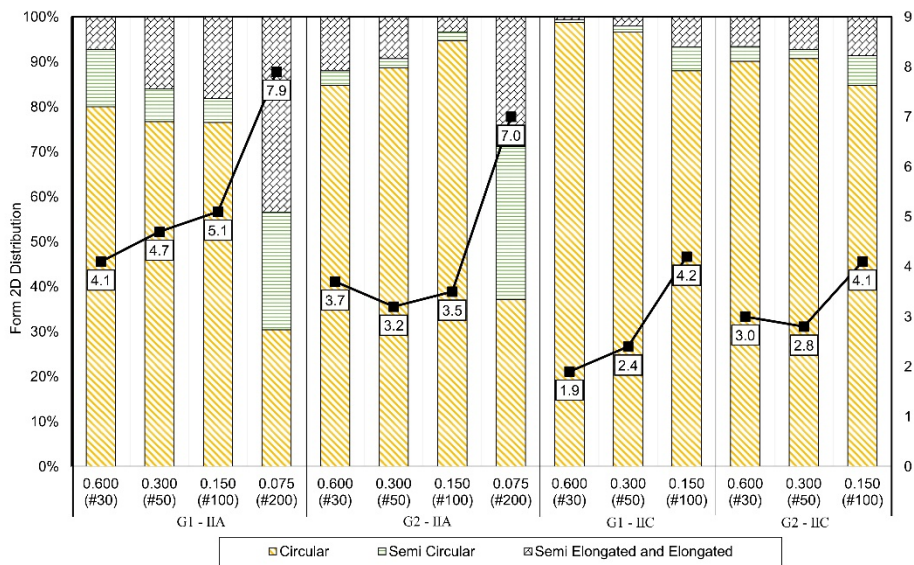
Researchers have been using Aggregate Image Measurement System (AIMS) for aggregates characterization (Masad et al., 2001; Al-Rousan, 2004; Diógenes et al, 2018, Ibiapino et al, 2020). To characterize the glass beads, the material was considered as fine aggregates (passing through sieve 4.750 mm). The test evaluated approximately 150 random particles retained at each one of sieves opening of 0.600mm, 0.300mm, 0.150mm and 0.075mm. The parameters evaluated were Form 2D and Gradient Angularity. Form 2D measures the particle elongation and its value ranges between zero (0) and twenty (20). As more elongated the particle is, its Form 2D value is approximately twenty (20). Gradient Angularity evaluates the particle angularity and it ranges from zero (0) to ten thousand (10,000). Angular particles present Gradient Angularity value is approximately 10,000 (Al-Rousan, 2004).

Table 1 summarizes the results for all glass beads. Both parameters were evaluated according to the classes proposed by Al-Rousan (2004) for aggregates from U.S.A. The Form 2D classes are Circular, Semi Circular, Semi Elongated and Elongated, and their ranges are from 0 to 6.5, 6.5 to 8.0, 8.0 to 10.5 and 10.5 to 20.0, respectively. The Angularity Index classes are Rounded, Semi Rounded, Sub Angular and Angular for the ranges of 0 to 2,100, 2,100 to 4,000, 4,000 to 5,400 and 5,400 to 10,000, respectively. Since the desirable classifications for glass beads are Circular and Rounded, the classes Semi Elongated and Elongated were grouped together for Form 2D evaluation, as well as Sub Angular and Angular for Angularity.

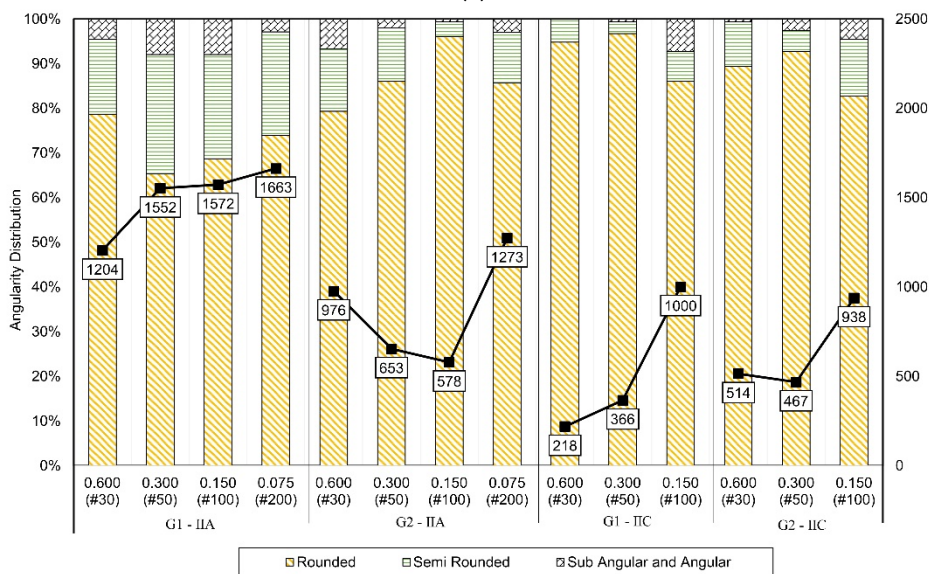
Table 1 presents the weighted average value of parameters. The results fit the classes Circular (Form 2D) or Rounded (Angularity), since these ranges classify spherical materials. G1 and G2 presented lower parameters' values for IIC than IIA, indicating the tendency of the larger particles (IIC) become more spherical. Regarding manufacturers, is notable how G2 parameters are closer to zero than G1 parameters for the IIA size showing the best shape characteristics, confirming the results obtained by the computerized optical equipment. The high values of standard deviation (SD) at Table 1 for all glass beads indicate large shape dispersion among the glass bead particles analyzed and the lack of control by manufacturers. Even so, the materials were analyzed considering the distribution of parameters at each sieve and the results are presented at Figure 5.

Table 1 – Glass bead AIMS results: Average and Standard Deviation Values

Glass bead	Type	Sieve	% retained	Form 2D		Angularity		
				Weighted Average	Standard Deviation	Weighted Average	Standard Deviation	
G1	IIA (70%)	0.600 (#30)	11.51	4.77	Circular	3.21	Rounded	1,501.08
		0.300 (#50)	65.77					
		0.150 (#100)	21.01					
		0.075 (#200)	1.71					
	IIC (30%)	0.600 (#30)	64.93	2.07	Circular	1.42	Rounded	691.75
		0.300 (#50)	33.56					
		0.150 (#100)	1.26					
		0.600 (#30)	11.32					
		0.300 (#50)	44.57					
		0.150 (#100)	39.14					
G2	IIA (70%)	0.600 (#30)	43.49	3.57	Circular	2.47	Rounded	1,033.97
		0.300 (#50)	54.29					
		0.150 (#100)	2.22					
		0.600 (#30)	11.32					
	IIC (30%)	0.300 (#50)	54.29	2.92	Circular	2.66	Rounded	993.23
		0.150 (#100)	2.22					



(a)



(b)

Figure 5. AIMS Results: (a) Distribution of Form 2D classes and average value by fraction; (b) Distribution of Angularity class and average value by fraction

Figure 5(a) displays the percentage of particles in each class and the average value represented by the black points considering the sieve for all glass beads regarding Form 2D. Regarding type IIA, the material retained at sieve #200 presented the major percentage of particles out of class Circular, which reduces the retroreflectivity. Other fractions presented a reasonable shape distribution, since over 80% particles were classified as Circular. For G1, the percentage of Circular particles decreases as the sieve opening decreases. In addition, the smaller fraction presented the higher Form2D average value for all beads. Type IIC had the percentage of Circular particles 13% higher than IIA, which reinforces that IIC could perform better than IIA for G1. For type IIA, G1 presented better shape parameters than G2, and for size IIC, the opposite occurred, in accordance with the thickness-to-length ratio results of computerized optical equipment CamSizer. The glass bead G1-IIA presented worst Form2D value than G2-IIA for all fractions, except for #200 in which both beads are equally bad. Regarding the average value of Form2D, G1-IIC, G2-IIC and G2-IIA have the lower value for the fraction with the major percentage of particles, which could indicate that the material was selected to improve the average shape characteristics. In addition, Form2D average values for fractions #30 and #50 of G2-IIC are very similar, around 3.0.

Figure 5(b) shows the percentage of particles in each class and the average value represented by the black points considering the sieve for all glass beads regarding Angularity Index. On contrary of Form 2D, the percentage of particles classified as Rounded does not present any trend correlated to the sieve size. In addition, all the fractions for all glass beads presented over 70% of particles as Rounded. As the other results showed, gradation IIC also presents better shape parameters than IIA for all the fractions analyzed. For all glass beads, the smaller fraction presented the worst average value of Angularity Index. Again, the glass beads which presented the worst shape parameters was G1-IIA, since all the average values of Angularity Index are closer to the superior limit of the class, as well as the fraction #0.075 for G2-IIA.

It is valid to highlight the difference between Form2D and Angularity Index, mainly because they represent different characteristics.

2.2.3. Technique's comparison

The parameters analyzed for both equipment have the same physical meaning, b/l and Form 2D evaluated the particle roundness for the area projected. SPHT and Angularity Index evaluated the angularity of particles. The characterization using AIMS takes more time than CamSizer but the results can be analyzed as function of each sieve size and be used as a tool to evaluate the manufacturing process since the result also present picture of each particles analyzed. The images are useful for a better understanding and technical controlling of the material before its use. In addition, AIMS classification range are adjusted for aggregates and not for glass beads, then further analysis must be carried out to adequate the range for glass beads.

Despite the difference on the mathematical formulations for parameters calculations, both devices measured properties of shape regarding elongation and angularity. Figure 6 correlates graphically the parameters. This research has no intention to correlate the techniques but discusses briefly if there is any connection between them.

By the results presented in Figure 6, the parameters evaluated by each equipment seems to present the same tendency. However, at Figure 6, the points correlating the measurement obtained from CamSizer and AIMS for G1-IIA are scattered when compared to other beads, especially for the correlation between Sphericity (CamSizer) and Angularity (AIMS). Compared

to Sphericity, the Angularity Index highlight the materials difference particularly due to its wider range. The large range to evaluate and classify the material contributes to the parameter sensibility and ability to differ the materials. Even though, the CamSizer is an accurate and fast method to evaluate glass beads.

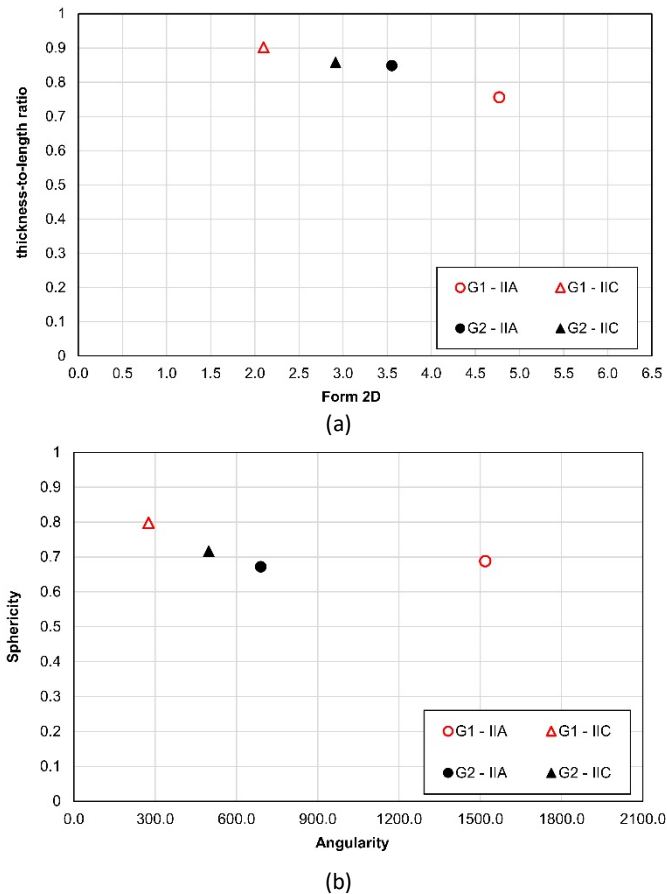


Figure 6. Comparison between parameters measured by CamSizer and AIMS: (a) thickness-to-length ratio and Form 2D; (b) Sphericity and Angularity

2.3. Paints

With intention to construct a test site to evaluate beads performance in the field, two white paints from different manufacturers were selected to minimize their influence on the results. Both binders were waterborne paints made of acrylic resin. The manufacturers did not inform about paints composition. The parameters evaluated for paints were: Viscosity, Storage Stability, No-Pick-Up Time, Specific Gravity, Gloss, Water, Flexibility and Solvent and Fuel Resistance and Abrasion, as recommended by ASTM D1155 (ASTM, 2015). Both paints were in accordance with the specification, allowing their use in the test site and the results were similar for both paints leading to expectation that both would perform similarly in the test site.

3. FIELD EXPERIMENT

3.1. Experimental design

The evaluation of paints and glass beads quality relied on the retroreflectivity monitoring of a test site for 11 months. The test site was constructed at BR-381, one important highway with

very heavy traffic ($N = 2.27 \times 10^7$ ESALs for 10-year project) in the Brazilian Southeastern region (Bosso et al, 2019). The design and the construction of the test site considered the recommendations and requirements of ASTM D713 (ASTM, 2012). Due to the high traffic volume of the highway, traffic interruptions for frequent retroreflectivity measurements would cause speed reduction and possible crashes. Therefore, the place selected for the test site construction was a toll plaza, since drivers are expecting the speed reduction at this section. Besides, the toll cabins allow the precisely traffic count. At the toll plaza, the pavement wearing course is an old dense-graded hot mix asphalt with smooth pavement surface texture.

The experiment compared all paints combined with all glass beads resulting in four different pavement marking materials' combinations: P1+G1, P1+G2, P2+G1, and P2+G2. The materials were applied by spray with the truck which dropped glass beads on the fresh paint. The application thickness of the fresh white paint was 0.5mm. The glass beads were applied in a total rate of 400g/m^2 in the application rate of 70% (280g/m^2) of gradation IIA and 30% (120g/m^2) of gradation IIC. The selection of paint thickness and glass beads application rate and density followed the Brazilian road agencies practices.

For each combination, there were two stripes painted transversally to traffic after the toll plaza cabin. The stripes width was 20 centimeters and their length was 13.8 meters which pass by three toll cabins. All the stripes suffered friction by vehicles' tire accelerating. The markings quality was evaluated by the retroreflectivity measured with a portable retroreflectometer (ASTM, 2011) for the period of 11 months. During this period, the retroreflectivity was measured 27 times including the value measured at the day of execution. The intervals between the measurements were random due to limitations on traffic interruption or wet surface caused by rain. In case of rain, the data collection was rescheduled to, at least, 24 hours after the rain stopped. The measurements were collected only during the day with dry surface. The retroreflectometer calibration followed the manufacturer recommendations before each measurement day.

The retroreflectivity was measured at points A and B for each cabin as presented in Figure 7. Points A and B represent the vehicles left and right-wheel-path, respectively. For each point, at all stripes and cabins, the retroreflectivity was measured twice. The retroreflectivity value for each combination at one specific cabin was the average of the two measurements at each point for both stripes and for both wheel-paths. The retroreflectivity value is different for each cabin since traffic and wear differ from cabin to cabin.

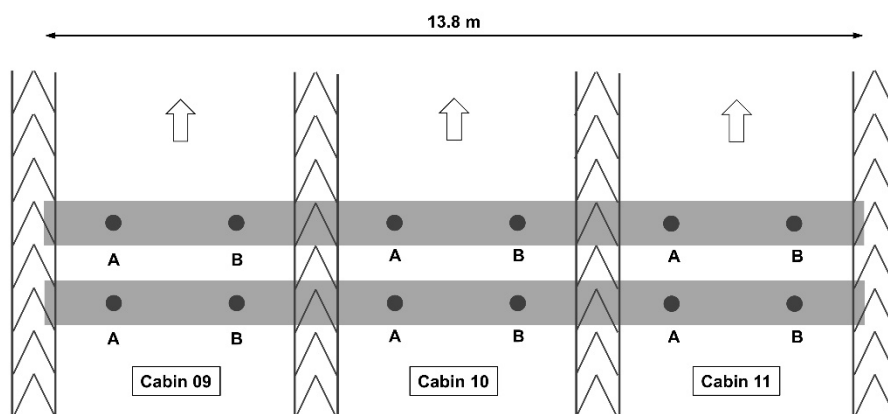


Figure 7. Points for retroreflectivity measurement

The traffic count could not consider the number of Equivalent Single Axle Load (ESAL) since such parameter considers the vehicles' weight and there was no weigh system near the tool plaza. In addition, the ESAL assumes that light vehicles have no influence on pavement markings degradation. Therefore, for this experiment, the traffic count was considered as number of accumulated axles, in which the vehicles (light or heavy) are counted only by their axles' quantity. It is important to highlight that one of the factors affecting pavement marking durability is the friction with vehicles' tire. The friction is different for light and heavy vehicle, but since there is no damage factor for this scenario, the authors assumed that both light or heavy vehicles with the same number of axles have the same impact on pavement marking.

3.2. Retroreflectivity degradation curve

Figure 8 shows the degradation curves for all combinations as function of accumulated axles. Since traffic varies from cabin to cabin, the accumulated traffic observed during the monitoring was separated in different ranges. The retroreflectivity value associated with each range was the average of all retroreflectivity value measured for any quantity of accumulated axles for the interval.

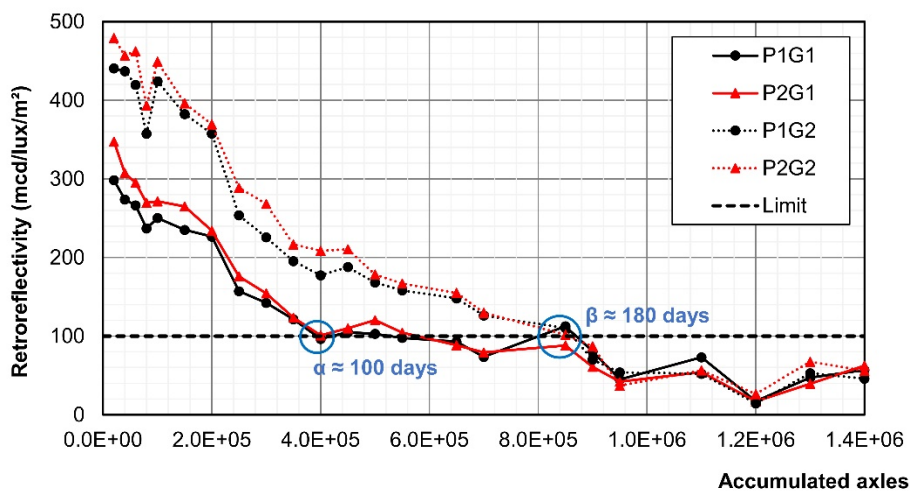


Figure 8. Retroreflectivity degradation curve over time

At Figure 8, the retroreflectivity degradation curves present the characteristic pattern for new markings described by Thamizharasan et al (2003) in which the retroreflectivity peak occurs within 15 to 45 days after painting. After the peak, the retroreflectivity decreases continually. Some other peaks are also observed and were attributed to after rain periods which combined to the traffic friction cause the cleaning effect on markings and increase the retroreflectivity value (Salles et al, 2015).

To evaluate the paints' performance, P1G1 must be compared to P2G1 and P1G2 must be compared to P2G2. For both scenarios, it is noticed that P2 performs better than P1, what cannot be properly explained considering the characterization according to ASTM D1155 (ASTM, 2015). The manufacturers did not inform the composition, but it is expected a higher pigment volume content for paint P2, which improves the abrasion resistance (Fatemi et al, 2006). This brings the question if the characterization presented is enough for evaluating the paints durability. Even though paints perform differently, glass beads were more influent for retroreflectivity.

By Figure 8 is possible to observe two groups of curves depending on glass bead's manufacturer, up to point β , where the curves overlap. The groups are associated to the influence of glass bead on pavement marking performance and can be evaluated by comparing combinations containing the same paint with different glass bead.

The results at Figure 8 show that combinations with G2 had retroreflectivity higher than combinations with G1, with average values 61% higher. Despite the difference on the retroreflectivity order of magnitude for G1 and G2, all curves follow the same trend for decrease, indicating that all combinations present similar glass bead loss. Regarding the minimum retroreflectivity recommended in Brazil, G1 reaches the limit value at 4.0×10^5 accumulated axles (point α) while glass bead G2 is acceptable until 8.2×10^5 accumulated axles (point β), indicating that G2 lasts twice the time than G1.

Considering the retroreflectivity degradation for the first 100 days, pavement markings with G1 decreased around 69% reaching the limit value, while G2 retroreflectivity decreased around 58%. When P1G2 and P2G2 reach the minimum retroreflectivity value accepted in Brazil, the retroreflectivity decreased 77%. Therefore, despite the elevated initial value of retroreflectivity for G2, the degradation rate of pavement markings with G1 and G2 are different.

The previously characterization of glass beads is useful for a better understanding of their field performance. Regarding the durability, the lack of adhesion coating of glass beads G2 did not affected their performance. By the granulometry, it is possible to note that glass beads G2 present a larger number of smaller particles for both gradations. Therefore, their embedment depth was enough to be retained by the binder film along time, while the larger particles of G1 are probably more easily removed from markings (Kalchbrenner, 1989; Miglitz, Fish and Graham, 1994).

In regard of retroreflectivity value, spherical particles lead to higher retroreflectivity (Smadi et al, 2014). The sample with the best shape properties was G1-IIC, while the worst bead was G1-IIA. The application rate of 70% of IIA and only 30% of IIC considers percentage by mass. Therefore, the number of particles of glass bead IIA is very large, since smaller beads have less mass and result in more particles. Consequently, even with the best shape properties among all beads, G1-IIC was not capable to improve pavement markings' retroreflectivity with G1 due to the small number of spherical particles in the whole set of glass beads G1. Regarding the glass beads G2, both gradations present satisfactory shape characteristics which corroborated the elevated retroreflectivity.

After all combinations reached the minimum required retroreflectivity in Brazil (point β), the curves do not follow any trend since the markings are aged and have lost many beads. The retroreflectivity value measurement depends on the reading area and some points may present a different amount and concentration of beads and the value measured is no longer trustful.

4. CONCLUSION

The pavement markings are complex road elements composed by glass beads and binders. They are highly exposed to traffic and weather. Thus, pavement marking durability varies according to the road where it is applied. This paper assessed the performance of a Brazilian glass beads G1 with recycled glass and an imported glass beads G2 with virgin glass by their size and shape evaluation, and by retroreflectivity degradation curve of pavement marking using two paints, P1 and P2.

Paints characterization by standards had no correlation to field performance since paints meet the standard specification. The glass bead's analysis using image tools was useful for a better understanding of the degradation curve of retroreflectivity and the performance of the materials in the field. Furthermore, it can also be used to evaluate the product quality and help to rank the materials before the field application.

The use of equipment as CamSizer is already prescribed by AASHTO and provides useful information of glass bead shape in a short period of time. AIMS is more time consuming compared to the CamSizer, but the analysis is done by fraction and provides more information which can be useful to better evaluate the material. The AIMS's class limits recommended for fine aggregates are inadequate to classify glass beads for pavement marking. AIMS uses statistical parameters as Average and Standard Deviation (SD) to characterize and classify the particles. For shape analysis, the SD is very interesting since it represents the variability of particles' physical properties. The elevated values of SD showed many particles outside the desirable classes.

Based on results, the Brazilian glass bead G1 presents satisfactory initial retroreflectivity values in the field, but present poor durability when compared to glass bead G2, what was explained by the shape analysis. Therefore, despite the advantage of cost and use of recycled material, the poor performance of G1 subjected to real conditions of traffic and weather would demand twice repainting than G2. The proper evaluation of materials characteristics to estimate field performance requires the analysis of shape, size, gradation, as well as the verification of adhesion coating. The procedure to characterize the materials helps to rank their quality and expected performance.

ACKNOWLEDGEMENTS

The authors would like to acknowledge CNPq, CAPES, ANTT, Arteris Concessionary and FAPESP for the financial support. The authors also acknowledge Arteris Concessionary (Autopista Fernão Dias) and Instituto Mauá de Tecnologia for the support on experimental tests and field monitoring.

REFERENCES

- AASHTO (2012) *TP 81-12 - Standard Method of Test for Determining Aggregate Shape Properties by Means of Digital Image Analysis*. American Association of State Highway and Transportation Officials, Washington, D.C., USA.
- AASHTO (2013a) *M247 - Standard Specification for Glass Beads Used in Pavement Markings*. Association of State Highway and Transportation Officials, Washington, D.C., USA.
- AASHTO (2013b) *PP74 - Standard Practice for Determination of Size and Roundness of Glass Beads Used in Traffic Markings by Means of Computerized Optical Method*. Association of State Highway and Transportation Officials, Washington, D.C., USA.
- ABNT (2013) *NBR 16184 - Horizontal roadmarking - Glass spheres and glass microspheres - Requirements and test methods*. Associação Brasileira de Normas Técnicas, Rio de Janeiro, Brazil.
- Al-Rousan, T. M. (2004) *Characterization of Aggregate Shape Properties Using a Computer Automated System*. PhD Dissertation. Texas A&M University. USA. DOI: <https://hdl.handle.net/1969.1/1485>
- ASTM (2011) *E1710 - Standard Test Method for Measurement of Retroreflective Pavement Marking Materials with CEN- Prescribed Geometry Using a Portable*. American Society for Testing Materials, West Conshohocken, PA, USA.
- ASTM (2012) *D713 - Standard Practice for Conducting Road Service Tests on Fluid Traffic Marking Materials*. American Society for Testing Materials, West Conshohocken, PA, USA.
- ASTM (2015) *D1155 - Standard Test Method for Roundness of Glass Spheres*. American Society for Testing Materials, West Conshohocken, PA, USA.
- Babic, D.; T. E. Burghardt and D. Babic (2015) Application and Characteristics of Waterborne Road Marking Paint. *International Journal for Traffic and Transport Engineering*, n.5, v.2, p. 150-169. DOI: [dx.doi.org/10.7708/ijtte.2015.5\(2\).06](https://doi.org/10.7708/ijtte.2015.5(2).06)
- Bosso, M.; K. L. Vasconcelos; L. L. Ho and L. L. B. Bernucci (2019) Use of Regression Trees to Predict Overweight Trucks from Historical Weigh-in-Motion Data. *Journal of Traffic and Transportation Engineering (English Edition)*. n.7, v.6, p. 843-859. DOI: doi.org/10.1016/j.jtte.2018.07.004
- Carlson, P. J.; E. S. Park and C. K. Andersen (2009) Benefits of Pavement Markings. *Transportation Research Record: Journal of the Transportation Research Board*, n. 2107, v. 1, p. 59-68. DOI: doi.org/10.3141/2107-06

- Diógenes, L. M.; I. S. Bessa; V. T. F. Castelo Branco and E. Mahmoud (2018) The Influence of Stone Crushing Processes on Aggregate Shape Properties. *Road Materials and Pavement Design*, n.20, v.4, p.877–894. DOI: doi.org/10.1080/14680629.2017.1422792
- Fatemi, S.; M. K. Varkani; Z. Ranjbar and S. Bastani (2006) Optimization of The Water-Based Road-Marking Paint by Experimental Design, Mixture Method. *Progress in Organic Coatings*, n.55, v.4, p.337–344. DOI: doi.org/10.1016/j.porgcoat.2006.01.006
- FHWA (2007) *Manual on Uniform Traffic Control Devices for Streets and Highways*. Federal Highway Administration, Washington, D.C., USA.
- Garboczi, E. and H. Azari (2011) Evaluating the Parameters of the Computerized Optical Method for Size and Roundness Measurement of Pavement Marking Glass Beads using X-ray Microtomography. In: *90th Annual Meeting of Transportation Research Board*. Washington DC, USA.
- Hummer, J. E.; W. Rasdorf and G. Zhang (2011) Linear Mixed-Effects Models for Paint Pavement-Marking Retroreflectivity Data. *Journal of Transportation Engineering*, n.137, v.10, p.705–716. DOI: doi.org/10.1061/(ASCE)TE.1943-5436.0000283
- Ibiapina, D. S.; L. M. Diógenes; V. T. F. Castelo Branco; S. M. Freitas; L. M. G. Motta. and D. F. Diógenes (2020) Análise estatística da qualidade das medidas das propriedades de forma de agregados com o uso do Processamento Digital de Imagens (PDI). *Transportes*, v. 28, n. 5, p. 1-12. DOI: doi.org/10.14295/transportes.v28i1.1865
- Kalchbrenner, J. (1989) Large Glass Beads for Pavement markings. *Transportation Research Record: Journal of the Transportation Research Board*, n.1230, p. 28–36. DOI: onlinepubs.trb.org/Onlinepubs/trr/1989/1230/1230-004.pdf
- Masad, E.; D. Olcott; T. White and L. Tashman (2001) Correlation of Fine Aggregate Imaging Shape Indices with Asphalt Mixture Performance. *Transportation Research Record: Journal of the Transportation Research Board*, n.1757, p. 148–156. DOI: doi.org/10.3141/1757-17.
- Migletz, J.; J. K. Fish and J. L. Graham (1994) *Roadway Delineation Practices Handbook*. Federal Highway Administration, Washington, D.C., USA.
- Migletz, J.; J. L. Graham; D. W. Harwood and K. M. Bauer (2001) Service Life of Durable Pavement Markings. *Transportation Research Record: Journal of the Transportation Research Board*, (1749), 13–21. DOI: doi.org/10.3141/1749-03
- Mizera, C.M. (2008) *Improving Pavement Marking Performance Through Contrasting New Methods to Quantify Marking Presence and Increasing Installation efficiencies through an Evaluation of Prototype Bead Guns*. Master Thesis. Iowa State University. Iowa, USA. DOI: doi.org/10.31274/rtd-180813-16415
- NTPEP (2004) *NTPEP Best Practices*. National Transportation Product Evaluation Program, Washington DC, USA.
- Pike, A. M. and P. Songchitrukka, P (2015) Predicting Pavement Marking Service Life with Transverse Test Deck Data. *Transportation Research Record: Journal of the Transportation Research Board*, n. 2482, p. 16–22. DOI: doi.org/10.3141/2482-03
- Rich, M.J.; R. E. Maki and M. J. Morena (2002) Development of a pavement marking management system: measurement of glass sphere loading in retroreflectivity pavement paints. *Transportation Research Record: Journal of the Transportation Research Board*, v. 1794, n. 1, p. 49-54. DOI: doi.org/10.3141/1794-06
- Salles, L. S.; D. S. Pereira; D. L. K. Teixeira and L. P. Specht (2015) Avaliação retrorrefletiva de pintura de demarcação horizontal: peculiaridades e considerações sobre a norma e os requisitos mínimos nacionais. *Transportes*, v. 23, n. 3, p. 6-17. DOI: doi.org/10.14295/transportes.v23i3.886
- Sathyanarayanan, S.; V. Shankar and E. T. Donnell (2008) Pavement Marking Retroreflectivity Inspection Data: A Weibull Analysis. *Transportation Research Record: Journal of the Transportation Research Board*, n. 2055, p. 63–70. DOI: doi.org/10.3141/2055-08
- Smadi, O.; N. Hawkins; B. A. Bektas; P. Carlson; A. Pike and C. Davies (2014) Recommended Laboratory Test for Predicting the Initial Retroreflectivity of Pavement Markings from Glass Bead Quality. *Transportation Research Record: Journal of the Transportation Research Board*, n. 2440, p. 94–102. DOI: doi.org/10.3141/2440-12
- Texas DOT (2004). *Pavement Marking Handbook*. Texas Department of Transportation, Texas, USA.
- Thamizharasan, A.; W. A. Sarasua and D. B. Clarke. (2003) A Methodology for Estimating the Lifecycle of Interstate Highway Pavement Marking Retroreflectivity. In: *83th Annual Meeting of Transportation Research Board*. Washington DC, USA.
- United Nations (2015) *The 2030 Agenda for Sustainable Development*. DOI: doi.org/10.1201/ b20466-7.
- WHO (2015) *Global Status Report on Road Safety 2015*. World Health Organization. Geneva, Switzerland. DOI: doi.org/http://www.who.int/violence_injury_prevention/
- WHO (2018) *Global Status Report on Road Safety 2018*. World Health Organization, Geneva, Switzerland.